Expanded View Figures

Figure EV1. MS/MS spectrum of peptides phosphorylated on S_{209}, S_{213}, S_{217}, and S_{221}.

A–D MS/MS spectrum of peptides phosphorylated on S_{209} (A), S_{213} (B), S_{217} (C), and S_{221} (D). The molecular weight of peptides is indicated on the right. Spectra are an assembly of ions produced by collision-induced dissociation of the precursor peptides. Fragmentation occurs preferentially at peptide bonds to generate b and y ions, which extend from the amino and carboxy terminus, respectively. The precursor peptide sequence and the different b and y ions identified in the spectrum are shown above. b and y ion peaks are shown in red and blue, respectively. b and y ions with the highest intensity are labeled on the spectrum. Neutral mass losses of H_2O, NH_3, and H_3PO_4 (P) are indicated. Analysis of y and b ion fragmentation patterns showed that S_{209} (A), S_{213} (B), S_{217} (C), and S_{221} (D) were phosphorylated *in vivo*.

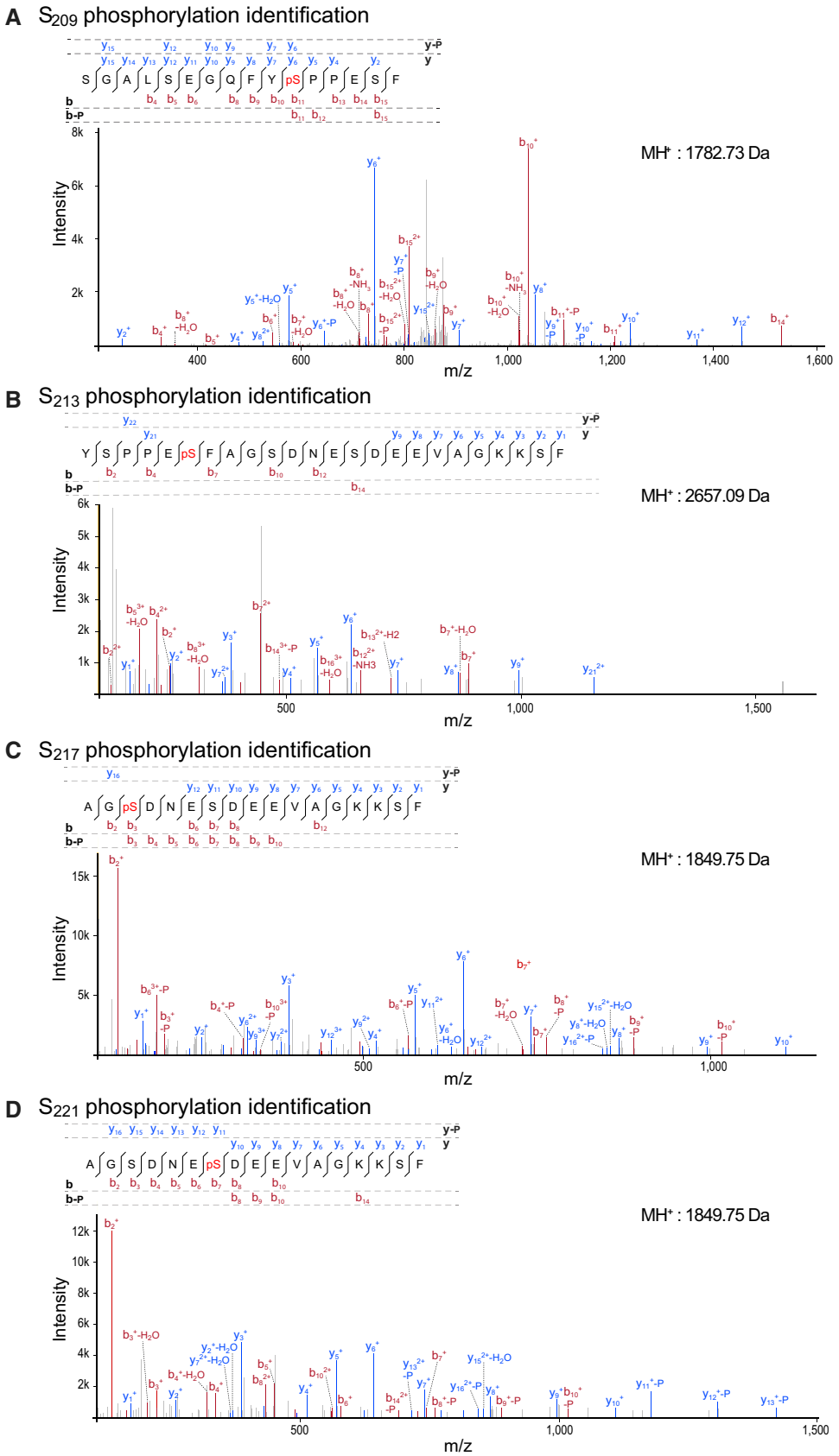
A S209 phosphorylation identification
S G A L S E G Q F Y pS P P E S F
MH+ : 1782.73 Da
Intensity
m/z
B S213 phosphorylation identification
Y S P P E pS F A G S D N E S D E E V A G K K S F
MH+ : 2657.09 Da
Intensity
m/z
C S217 phosphorylation identification
A G pS D N E S D E E V A G K K S F
MH+ : 1849.75 Da
Intensity
m/z
D S221 phosphorylation identification
A G S D N E pS D E E V A G K K S F
MH+ : 1849.75 Da
Intensity
m/z

Figure EV1.

Figure EV2. Interaction of VAP-A, VAP-B, and MOSPD2 with the Phospho-FFAT of STARD3.

A Interaction of VAP-A K50L, VAP-B K43L, and MOSPD2 K363L mutants with conventional and Phospho-FFAT motif. Wild-type and mutant MSP domains were pulled down with phosphorylated STARD3 (pS_{209} + pS_{213}), ORP1 FFAT peptides, and with the negative control peptide. The input fraction corresponds to the recombinant proteins used in the assay. Input and bound proteins were revealed by Coomassie Blue staining. Note that lysine K50 in VAP-A and K43 in VAP-B are required for the interaction with a Phospho-FFAT, and not with a conventional FFAT.

B Interaction of VAP-A, VAP-B, MOSPD2 with phosphomimetic STARD3 Phospho-FFAT motif. Wild-type and mutant MSP domains were pulled down with unphosphorylated, phosphorylated (pS_{209}), phosphomimetic ($S_{209}D$ and $S_{209}D/P_{210}A$), and with the negative control peptide. The input fraction corresponds to the recombinant proteins used in the assay. Input and bound proteins were revealed by Coomassie Blue staining. Acidic (D) or phosphorylated residues (pS), and alcoholic (S) residues are in red and green, respectively; the other residues are in black.

C STARD3 and VAP-A/VAP-B or MOSPD2 complex formation requires a unique phosphorylation of the Phospho-FFAT motif. Western blot analysis of proteins pulled down using the peptides described in Fig EV3A. The input fraction corresponds to the HeLa cell total protein extract. Streptavidin beads were first coupled to the indicated biotinylated peptides, or left without peptide (ø). The soluble fraction after the incubation of the protein extract with the beads (Unbound; left), and proteins attached to the beads (Bound; right) were analyzed by Western blot using anti-VAP-A, anti-VAP-B, and anti-MOSPD2 antibodies. Actin was used as a loading control.

D Immunoprecipitation (GFP-Trap) experiments between GFP-tagged VAP-A and Flag-tagged STARD3 (WT and $P_{210}A$ mutant). Approximatively 15 μg of total protein extract was analyzed by Western blot using anti-STARD3, anti-GFP, and anti-Actin antibodies. Immunoprecipitated material was analyzed using anti-STARD3 and anti-GFP antibodies.

Source data are available online for this figure.

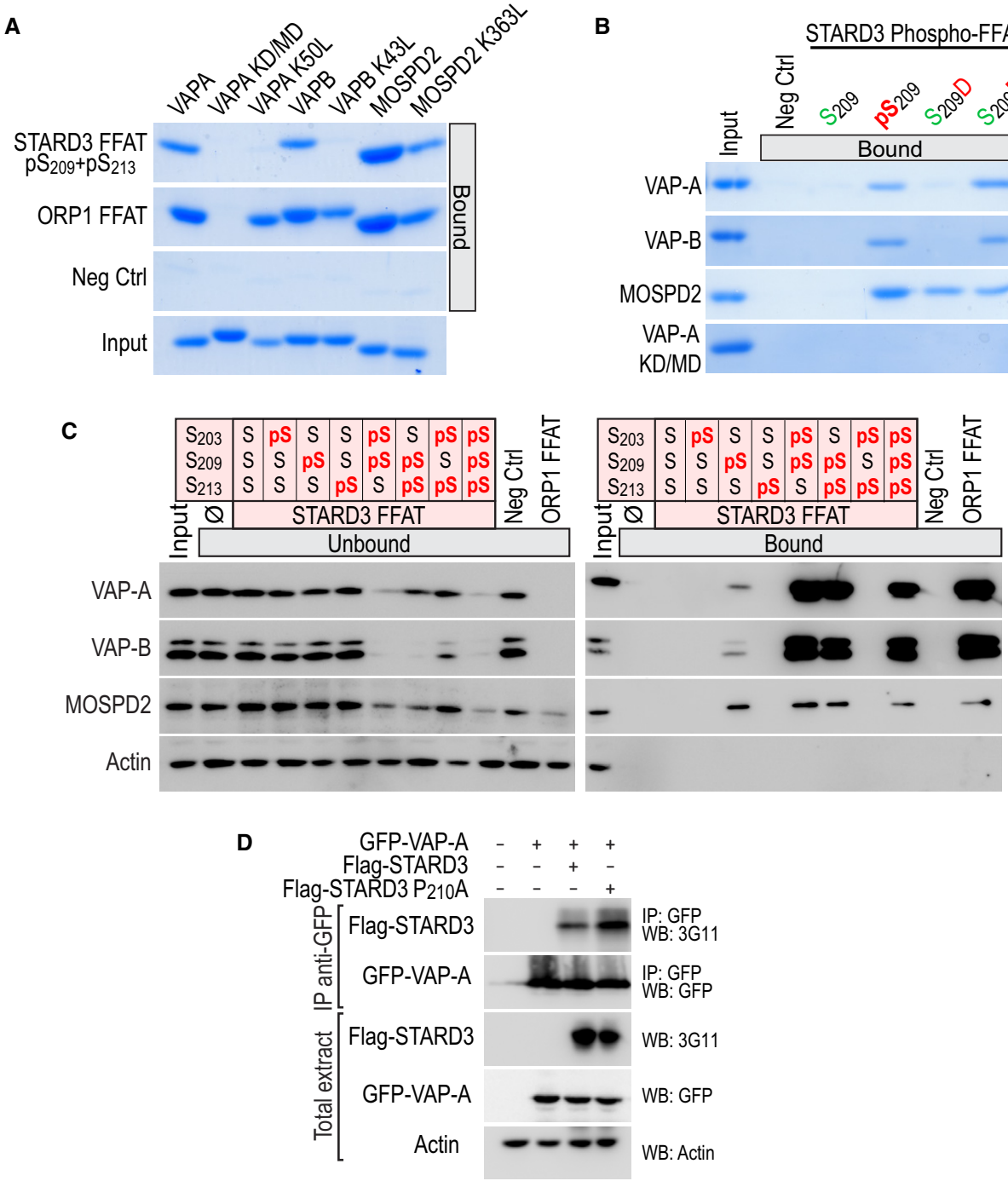
A
VAPA
VAPA KD/MD
VAPA K50L
VAPB
VAPB K43L
MOSPD2
MOSPD2 K363L
STARD3 FFAT pS209+pS213
ORP1 FFAT
Neg Ctrl
Input
Bound
B
STARD3 Phospho-FFAT
Input
Neg Ctrl
S209
pS209
S209D
S209D/P210A
Bound
VAP-A
VAP-B
MOSPD2
VAP-A KD/MD
C
S203
S209
S213
STARD3 FFAT
Input
Ø
Neg Ctrl
ORP1 FFAT
Unbound
Bound
VAP-A
VAP-B
MOSPD2
Actin
D
GFP-VAP-A
Flag-STARD3
Flag-STARD3 P210A
IP anti-GFP
Total extract
Flag-STARD3
GFP-VAP-A
Actin
IP: GFP WB: 3G11
IP: GFP WB: GFP
WB: 3G11
WB: GFP
WB: Actin

Figure EV2.

Figure EV3. The MSP domain of VAP-A/VAP-B/MOSPD2 binds the phosphorylated Phospho-FFAT with an affinity in the micromolar range.

A Sequence of the peptides used for SPR and the pull-down assays. The peptides are composed of an amino-terminal biotin, a linker sequence (GAMR) and the FFAT sequence of STARD3 (residues 200–216) either without phosphorylated serine or with combinations of phosphorylated serines (positions 203, 209, and 213 in STARD3 protein). The core FFAT sequence (residues 1–7) is highlighted in red. ORP1 FFAT peptide corresponding to residues 469–485 (Accession Number Q9BXW6-1), and a random sequence (control peptide) are used as positive and negative control, respectively. Acidic (D and E) or phosphorylated serine (pS), alcoholic (S and T), and aromatic (F, W, and Y) residues are in red, green and blue, respectively; the other residues are in black.

B–D SPR analysis of the MSP domain of VAP-A binding onto immobilized ORP1 FFAT peptide (B), pS_{203} (C) or pS_{203} + pS_{209} + pS_{213} (D) STARD3 FFAT peptides. Representative sensorgrams resulting from the interaction between the MSP domain of VAP-A injected at different concentrations and the different STARD3 FFAT peptides are shown in (B left), (C), and (D left). Binding curves display the SPR signal (RU) as a function of time. Concentrations printed in bold indicate samples measured twice. Steady-state analysis of the interaction between ORP1 FFAT (B right) and pS_{203} + pS_{209} + pS_{213} (D right) STARD3 FFAT peptide and the MSP domain of VAP-A. Equilibrium responses (R_{eq}) extracted from the left panel were plotted as a function of the dimeric MSP domain of VAP-A concentration, and fitted with a Langmuir binding model.

E Interaction dissociation constants between the different FFAT peptides and the MSP domains of VAP-A, VAP-B, and MOSPD2. MSP concentrations are expressed as dimer for VAP-A and VAP-B, and monomer for MOSPD2. The different ionic strengths correspond to the following buffers (pH 7.5): low: 20 mM Tris–HCl, 75 mM NaCl; medium: 50 mM Tris–HCl, 75 mM NaCl; high: 50 mM Tris–HCl, 300 mM NaCl. Buffers were supplemented with P20 (0.005% *v/v*). ND: not determined. Mean values of *n* independent experiments: $n = 2$ for pS_{209}, pS_{209} + pS_{213}, and pS_{203} + pS_{209} + pS_{213} (high); 4 for pS_{203} + pS_{209} + pS_{213} (low), ORP1 (low and high), and pS_{203} + pS_{209} + pS_{213} (medium) with MOSPD2; 6 for pS_{203} + pS_{209} + pS_{213} (medium) with VAP-A and VAP-B; 12, 11, and 7 for ORP1 (medium) with VAP-A, VAP-B, and MOSPD2, respectively. Uncertainties are obtained from the standard deviation considering a *t*-distribution coefficient for a risk factor of 32%.

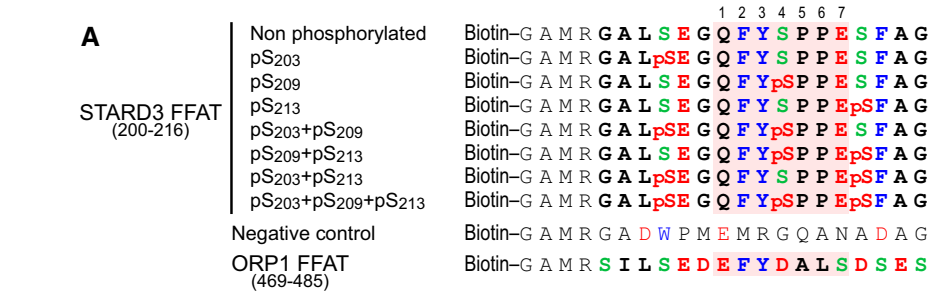

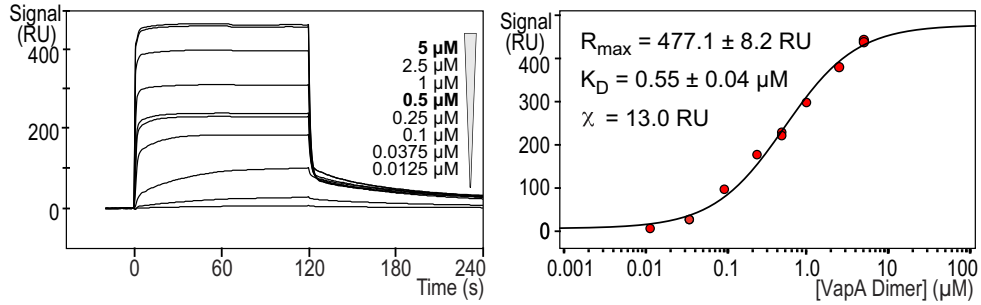

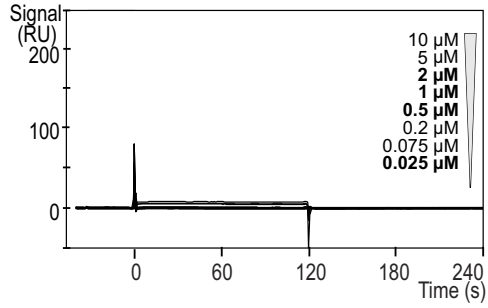

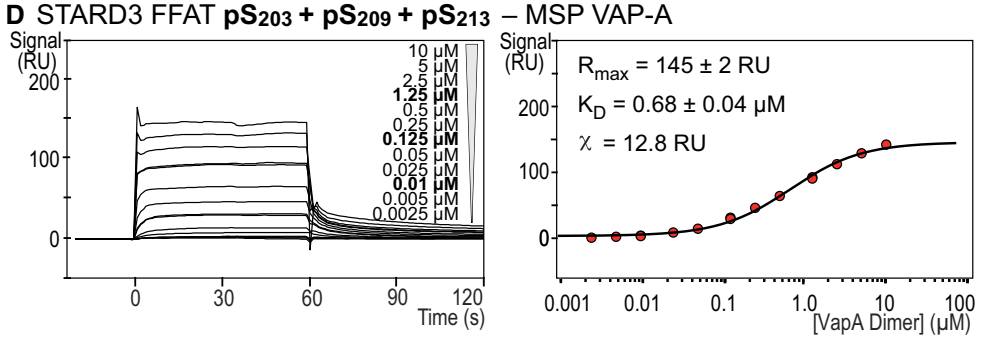

E Effect of ionic strength on interaction dissociation constants ($K_D \pm \Delta K_D$)

		Ionic strength	MSP domain		
			VAP-A	VAP-B	MOSPD2
STARD3 FFAT Peptide	pS209	Low	1.50 ± 0.17 µM	2.11 ± 0.19 µM	0.41 ± 0.41 µM
		Medium	5.62 ± 0.30 µM	7.14 ± 0.39 µM	1.14 ± 0.30 µM
		High	ND	ND	ND
	pS209+pS213	Low	0.79 ± 0.10 µM	1.38 ± 0.14 µM	0.18 ± 0.24 µM
		Medium	3.56 ± 0.22 µM	4.78 ± 0.25 µM	0.35 ± 0.16 µM
		High	ND	ND	ND
	pS203+pS209+pS213	Low	0.17 ± 0.02 µM	0.23 ± 0.09 µM	0.02 ± 0.01 µM
		Medium	0.77 ± 0.06 µM	1.59 ± 0.28 µM	0.16 ± 0.04 µM
		High	29.1 ± 0.5 µM	16.10 ± 0.64 µM	ND
ORP1 FFAT Peptide		Low	0.16 ± 0.01 µM	0.20 ± 0.06 µM	0.10 ± 0.02 µM
		Medium	0.54 ± 0.05 µM	0.80 ± 0.06 µM	0.63 ± 0.11 µM
		High	14.2 ± 2.5 µM	11.3 ± 1.5 µM	ND

Figure EV3.

Figure EV4. Effect of non-phosphorylatable and phosphomimetic mutations of S_{209} on the formation of ER-endosome contacts involving VAP-B *in vivo*.

A–D GFP-VAP-B (A–D; green)-expressing cells were left untransfected (A) or transfected with Flag-STARD3 (B), Flag-STARD3 S_{209}A (C), and Flag-STARD3 S_{209}D/P_{210}A (D), and labeled using anti-Flag (magenta) antibodies. The subpanels on the right are higher magnification (3.5×) images of the area outlined in white. The Overlay panel shows merged green and magenta images. The Coloc panel displays a colocalization mask on which pixels where the green and the magenta channels co-localize are shown in white. Scale bars: 10 μm. Inset scale bars: 2 μm.

E Pearson's correlation coefficients between VAP-B (WT and KD/MD) and STARD3 (WT, S_{209}A, S_{209}D, S_{209}D/P_{210}A or FA/YA mutants) staining are shown. Each dot represents a single cell (number of cells: VAP-B–STARD3: 20; VAP-B–STARD3 S_{209}A: 18; VAP-B–STARD3 S_{209}D: 27; VAP-B–STARD3 S_{209}D/P_{210}A: 26; VAP-B–STARD3 FA/YA: 21; VAP-B KD/MD–STARD3: 21, from at least three independent experiments). Means and error bars (SD) are shown. Kruskal–Wallis with Dunn's multiple comparison test (**$P < 0.01$; ***$P < 0.001$).

F Top: Western blot analysis of protein extracts from HeLa cells transfected with control siRNAs (siCtrl) and siRNAs targeting STARD3 (siSTARD3) using anti-STARD3 and anti-Actin antibodies. Bottom: After siRNA transfection, the cells were transfected with GFP-VAP-A and STARD3 (WT, STARD3 S_{209}A, and STARD3 S_{209}D/P_{210}A). STARD3 expression vectors contained a cDNA with silent mutations rendering it insensitive to siRNAs. The cells were labeled using anti-STARD3 antibodies. Pearson's correlation coefficients between STARD3 (WT, STARD3 S_{209}A, and STARD3 S_{209}D/P_{210}A) and VAP-A staining are shown. Note that the colocalization between VAP-A and STARD3 is similar in the presence and absence of endogenous STARD3. Means and error bars (SD) are shown. Kruskal–Wallis with Dunn's multiple comparison test (ns: $P \geq 0.05$).

Source data are available online for this figure.

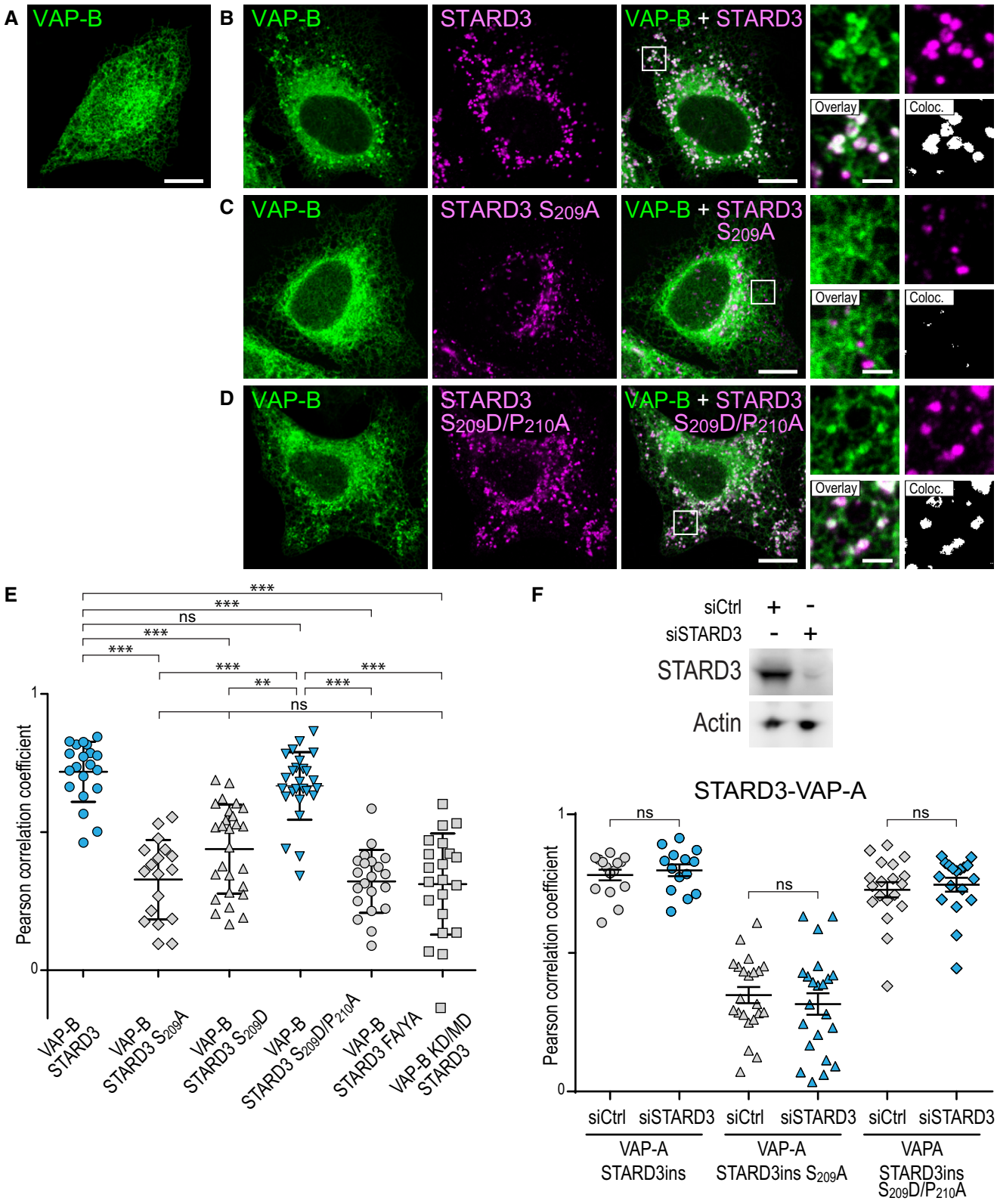
A
VAP-B
B
VAP-B
STARD3
VAP-B + STARD3
Overlay
Coloc.
C
VAP-B
STARD3 S209A
VAP-B + STARD3 S209A
Overlay
Coloc.
D
VAP-B
STARD3 S209D/P210A
VAP-B + STARD3 S209D/P210A
Overlay
Coloc.
E
Pearson correlation coefficient
1
0
***
***
ns
***
***
***
***
**
***
ns
VAP-B STARD3
VAP-B STARD3 S209A
VAP-B STARD3 S209D
VAP-B STARD3 S209D/P210A
VAP-B STARD3 FA/YA
VAP-B KD/MD STARD3
F
siCtrl + -
siSTARD3 - +
STARD3
Actin
STARD3-VAP-A
Pearson correlation coefficient
1
0
ns
ns
ns
ns
siCtrl siSTARD3 siCtrl siSTARD3 siCtrl siSTARD3
VAP-A STARD3ins
VAP-A STARD3ins S209A
VAPA STARD3ins S209D/P210A

Figure EV4.

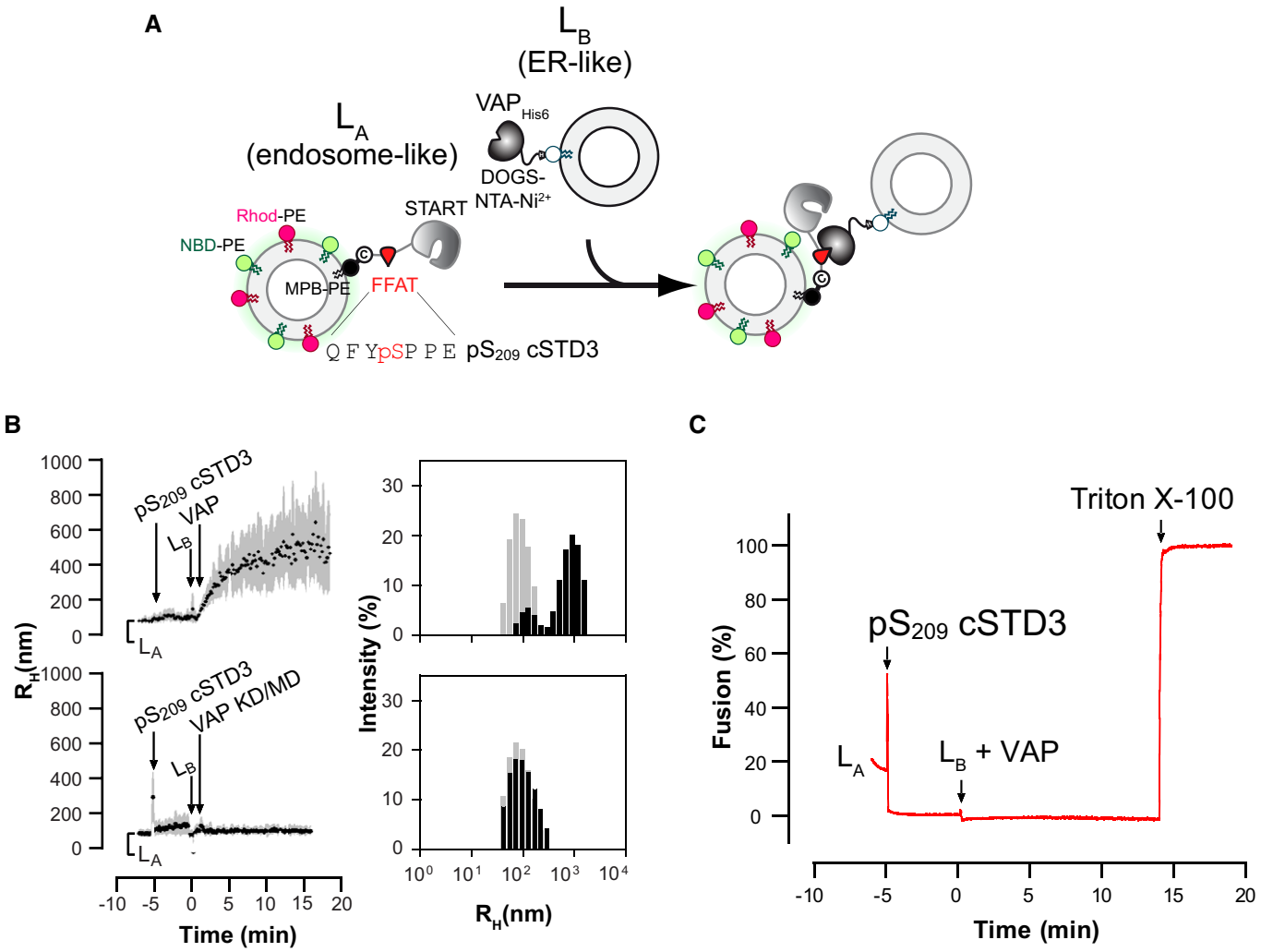

Figure EV5. The attachment of liposomes by pS_{209} cSTD3 does not induce membrane fusion.

A Description of the experimental strategy. L_A liposomes (endosome-like) are decorated with pS_{209} cSTD3 owing to covalent links with MPB-PE (1,2-dioleoyl-*sn*-glycero-3-phosphoethanolamine-N-[4-(p-maleimidophenyl) butyramide]), and mixed with L_B liposomes (ER-like) covered by VAP-A_{His6} attached to DOGS-NTA-Ni^{2+} (1,2-dioleoyl-sn-glycero-3-[(N-(5-amino-1-carboxypentyl) iminodiacetic acid) succinyl]; nickel salt). L_A liposomes contain the FRET pair NBD-PE (1,2-dioleoyl-*sn*-glycero-3-phosphoethanolamine-N-(7-nitro-2-1,3-benzoxadiazol-4-yl)) and Rhod-PE (1,2-dioleoyl-*sn*-glycero-3-phosphoethanolamine-N-(lissamine rhodamine B sulfonyl)). The fusion of L_A and L_B liposomes is followed by measuring an increase in NBD-PE fluorescence, which is initially quenched due to FRET with Rhod-PE. The percentage of fusion is equal to $100 \times ((F - F_0)/(F_{max} - F_0))$ where F_0 is the signal measured before the addition of L_B liposomes decorated with VAP-A_{His6}, and F_{max} is the signal measured after adding Triton X-100 (1% *v/v* final concentration).

B Aggregation assays. L_A liposomes (50 μM total lipids) were incubated for 5 min with pS_{209} cSTD3 (380 nM). Then, L_B liposomes (50 μM total lipids) and VAP-A_{His6} or VAP-A $(KD/MD)_{His6}$ (700 nM) were successively added. *Left panels*: mean radius (black dots) and polydispersity (shaded area) over time. *Right panels*: size distribution before (gray bars) and after the reaction (black bars).

C Fusion assay. DOPC (1,2-dioleoyl-*sn*-glycero-3-phosphocholine) liposomes (62.5 μM total lipids, L_A) containing 3 mol% MPB-PE, 1% NBD-PE, and 1% Rhod-PE were mixed with pS_{209} cSTD3 (475 nM). After 5 min, liposomes (DOPC/DOGS-NTA-Ni^{2+} 90/10 mol/mol, 62.5 μM total lipids, L_B), covered or not with 1 μM of VAP-A_{His6}, were added. At the end of the experiment, Triton X-100 was added (1% *v/v* final concentration) to disrupt liposomes and eliminate energy transfer, allowing the determination of the maximal fluorescence of NBD-PE that would be measured for a complete membrane fusion.